ELSEVIER

Surface Science 410 (1998) 200–213

surface science

A temperature programmed desorption study of the reaction of methylacetylene on Pt(111) and Sn/Pt(111) surface alloys

John W. Peck, Daniel I. Mahon, Bruce E. Koel *

Department of Chemistry, University of Southern California, Los Angeles, CA 90089-0482, USA

Received 19 August 1997; accepted for publication 2 March 1998

Abstract

The adsorption and reaction of methylacetylene ($H_3CC{\equiv}CH$) on Pt(111) and the p(2×2) and ($\sqrt{3}\times\sqrt{3}$)R30°−Sn/Pt(111) surface alloys were investigated with temperature programmed desorption, Auger electron spectroscopy and low energy electron diffraction. Hydrogenation of methylacetylene to form propylene is the most favored reaction pathway on all three surfaces accounting for ca 20% of the adsorbed monolayer. Addition of Sn to the Pt(111) surface to form these two ordered surface alloys suppresses the decomposition of methylacetylene to surface carbon. The alloy surfaces also greatly increase the amount of reversibly adsorbed methylacetylene, from none on Pt(111) to 60% of the adsorbed layer on the ($\sqrt{3}\times\sqrt{3}$)R30°−Sn/Pt(111) surface alloy. Methylacetylene reaction also leads to a small amount of desorption of benzene, along with butane, butene, isobutylene and ethylene. There is some difference in the yield of these other reaction products depending the Sn concentration, with the (2×2)-Sn/Pt(111) surface alloy having the highest selectivity for these. Despite previous experiments showing cyclotrimerization of acetylene to form benzene on the Pt–Sn surface alloys, the analogous reaction of methylacetylene on the alloy surfaces was not observed, that is, cyclotrimerization of methylacetylene to form trimethylbenzene. It is proposed that this and the high yield of propylene is due to facile dehydrogenation of methylacetylene because of the relatively weak H–CH_2CCH bond compared to acetylene. The desorption of several C_4 hydrocarbon products at low (<170 K) temperature indicates that some minor pathway involving C–C bond breaking is possible on these surfaces.

Keywords: Alkynes; Alloys; Auger electron spectroscopy; Chemisorption; Low energy electron diffraction; Low index single crystal surfaces; Platinum; Single crystal surfaces; Thermal desorption; Thermal desorption spectroscopy; Tin

1. Introduction

The cyclotrimerization of alkynes has been the subject of intense research since Berthelot first reported the formation of benzene from acetylene over 125 years ago [1]. Many studies of this reaction on single crystal surfaces under ultrahigh vacuum (UHV) conditions (Ni [2], Cu[3] Pd [4–17]) have been carried out. The extensive study of this reaction by Lambert over Pd has established the acetylene cyclotrimerization mechanism on Pd(111) in some detail. This reaction is believed to proceed through a metallocyclopentadiene intermediate with no cleavage of either C–C or C–H bonds. In this mechanistic scheme the reaction begins with the coordination of two alkynes to an active metal site, then a cyclization to form the metallocycle, and finally the addition of a third alkyne to form the aromatic product [10,17]. This basic mechanism has also been observed for a number of alkynes, including methylacetylene, on TiO_2 [18].

* Corresponding author. Fax: 1 213 740 3972;
e-mail: koel@chem1.usc.edu

0039-6028/98/$19.00
PII: S0039-6028(98)00252-0

In contrast to Pd, Pt does not show any reactivity for the cyclotrimerization of alkynes under UHV conditions. Acetylene adsorbed on Pt(111) disproportionates to form a bridging ethylidyne and unidentified residues (possibly CCH) which decompose further as the temperature is increased to form surface carbon and gas-phase hydrogen by 800 K. The authors' group has studied the effects that alloying Sn with the Pt(111) surface have on the reactivity of Pt(111) towards the decomposition of saturated and unsaturated hydrocarbons. For example, it was shown that simple organic molecules adsorbed on Sn/Pt(111) alloys have greatly reduced reactivity toward dehydrogenation and decomposition [19,20]. Attracted by the reduced reactivity of these alloys, the adsorption of acetylene was examined and it was reported that the decomposition of acetylene is substantially reduced and one result is that the cyclotrimerization of acetylene to benzene is promoted [21]. It was found that both benzene and butadiene (a probable product of the hydrogenation of a C_4 metallocycle intermediate) desorbed below 400 K in temperature programmed desorption (TPD) after adsorption of acetylene on the Sn/Pt(111) surface alloys.

This report examines the adsorption and reaction of methylacetylene on Pt(111) and the Sn/Pt(111) surface alloys. It is found that the decomposition of methylacetylene is strongly suppressed with an increasing concentration of Sn alloyed in the Pt(111) surface. However, a trimethylbenzene product from a cyclotrimerization reaction was not observed, and instead propylene is the principal reaction product desorbed.

2. Experimental

Experiments were performed in a stainless steel UHV chamber equipped with instrumentation for Auger electron spectroscopy (AES), low energy electron diffraction (LEED) and Ar^+ ion sputtering. A shielded UTI 100C quadrupole mass spectrometer (QMS) was used for TPD. The system base pressure was 5×10^{-11} Torr. AES spectra were recorded using a Perkin–Elmer (15-255G) cylindrical mirror analyzer (CMA). LEED was carried out using Perkin–Elmer (15-180) LEED optics. All TPD measurements were made using the QMS in line-of-sight with the sample surface and using a linear heating rate of ~4 K s^{-1}. In this procedure, the crystal was positioned ~1 mm from the entry aperture of the QMS shield to reduce contributions to the spectra from the crystal back and edges [22]. A screen biased at -55 V was placed between the QMS and the crystal to eliminate possible damage to the adsorbed layer from low energy electrons coming from the QMS ionizer region [23].

The Pt(111) crystal could be cooled to 95 K using liquid nitrogen or resistively heated to 1200 K. The temperature was recorded by a chromel–alumel thermocouple spot welded to the side of the crystal. The Pt(111) crystal was cleaned using the procedure found in Ref. [24]. Preparation of the Pt–Sn surface alloys was achieved by evaporating 1–3 monolayers (ML) of Sn on the clean Pt(111) substrate surface followed by annealing the sample to 1000 K for 10 s. Depending upon the initial Sn dose, the annealed surface exhibited either a $p(2\times2)$ or $(\sqrt{3}\times\sqrt{3})R30^\circ$ LEED pattern [25]. It has now been confirmed that these patterns correspond to the (111) face of a Pt_3Sn alloy and a substitutional alloy of composition Pt_2Sn, respectively, rather than Sn adatoms [26]. Angle-dependent low energy ion scattering spectroscopy (LEISS) measurements using 500–1000 eV Li^+ showed that the Sn atoms are almost coplanar with the Pt, protruding $\sim0.022\pm0.005$ nm above the surface in a monolayer surface alloy [27]. LEED *I–V* calculations [28] and X-ray forward scattering [29] have recently confirmed these results. For simplicity the $p(2\times2)$ and $(\sqrt{3}\times\sqrt{3})R30^\circ-Sn/Pt(111)$ surface alloys will be referred to in this paper as the (2×2) and $\sqrt{3}$ alloys, respectively. A diagram of these surfaces is provided in Fig. 1.

Methylacetylene (Aldrich, Milwaukee, WI, 97%) was purified by freeze–pump–thaw cycles. The purity was checked by in situ mass spectrometry. Gas exposures for the TPD studies were given with the sample at a temperature below 100 K. Exposures are given in units of Langmuirs (10^{-6} Torr·s) after the measured values were

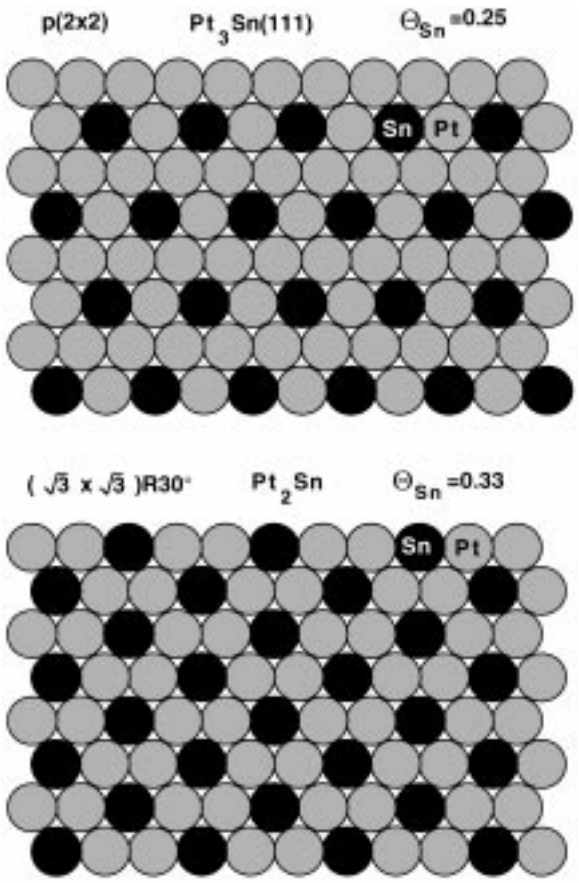

Fig. 1. Schematic top view of the structure of two Sn/Pt(111) surface alloys.

multiplied by a factor to account for the multicapillary array doser enhancement and divided by an additional factor of 6 [30] to correct for the ion gauge sensitivity. The doser correction factor was obtained by comparing uptake curves from exposures produced by the directed beam doser with those from background exposures. Because of the carbon contamination resulting from C_3H_6 TPD experiments on clean Pt(111), the surface must be cleaned following each experiment. The carbon contamination was removed by heating the surface to 800 K in 2×10^{-8} Torr O_2 for 10–15 min and then flash annealing to 1000 K in vacuum. The cleanliness and long-range order of all surfaces were checked using AES and LEED prior to each experiment. In addition, the alloy surfaces were checked with LEED following each TPD experiment to assure no irreversible adsorbate induced reconstruction occurred.

3. Results

3.1. Methylacetylene adsorption, desorption and decomposition

Fig. 2 shows methylacetylene TPD spectra following methylacetylene adsorption on Pt(111) and the two Pt–Sn surface alloys for a variety of exposures. Exposure of methylacetylene on the Pt(111) surface leads to irreversible adsorption of the chemisorbed molecule and no molecular desorption occurs >200 K. Peaks appear at higher coverages at 138 and 114 K that are assigned to desorption of a physisorbed second layer (on top of the chemisorbed monolayer) and multilayers of methylacetylene, respectively. This lowest temperature peak does not saturate up to exposures of over 30 L. Both alloys also have these two low temperature peaks, as observed in the Pt(111) spectra, but these are not shown here. The (2×2) alloy shows three high temperature methylacetylene desorption peaks in TPD, and these three peaks at 370, 460 and 510 K are associated with monolayer states of chemisorbed methylacetylene. Evolution of methylacetylene is observed at very low exposures. The $\sqrt{3}$ alloy shows only a single intense high temperature desorption peak at 370 K associated with desorption of a chemisorbed state of methylacetylene. On both alloys, no significant shift in the position of these high temperature methylacetylene desorption peaks with increasing coverage was seen.

Previous studies of ethylene, propylene [31] and acetylene [21] on Pt(111) and the Pt–Sn alloys have determined the chemisorbed monolayer coverage of these molecules to be 0.25, 0.25 and 0.27 ML, respectively, independent of the concentration of Sn in the surface alloy. Because of the similar size and chemical nature of methylacetylene, it will be assumed for the rest of this paper that the monolayer coverage of methylacetylene is 0.25 ML on all three surfaces. This assumption is

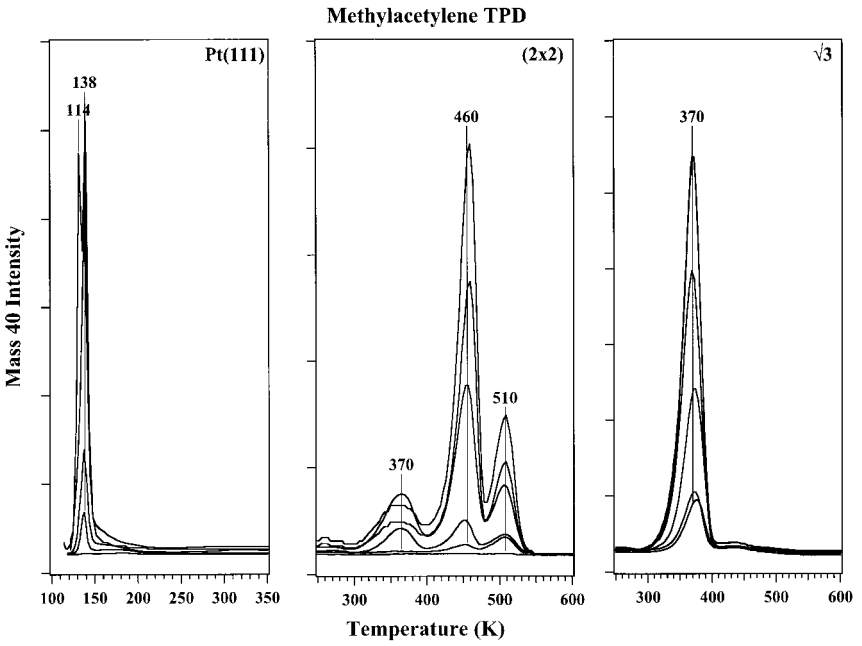

Fig. 2. Methylacetylene TPD for a series of coverages on the Pt(111), (2×2) and $\sqrt{3}$ Sn/Pt(111) surface alloys at 108 K.

supported by measurements of the C/Pt ratio in AES after dosing and a mass balance on the desorbed products in TPD.

In a comparison of the results from Fig. 2, TPD spectra are presented in Fig. 3 for methylacetylene desorption after an exposure of methylacetylene to give slightly greater than monolayer coverage on the Pt(111) and Sn/Pt(111) surface alloys. In this figure, the intensity scale and thus absolute peak areas and adsorbate coverages, are directly comparable for the three surfaces. Alloying Sn in the Pt(111) surface causes some reversible adsorption of the chemisorbed monolayer and increasing the concentration of Sn significantly reduces the activation energy for methylacetylene desorption. On the (2×2) surface alloy, three molecular methylacetylene peaks were observed at 370, 460 and 505 K that correspond to desorption activation energies of 23, 28.5 and 31 kcal mol^{-1} using Redhead analysis [32]. On the $\sqrt{3}$ surface alloy, methylacetylene's TPD spectra is dominated by a single peak at 370 K which has a desorption activation energy of 23 kcal mol^{-1}. In addition to lowering the desorption activation energy, increasing the concentration of Sn increases the amount of reversible adsorption by a factor of 2. The area under the methylacetylene TPD peaks correspond to desorption of 0.06 ML or 26% of the chemisorbed methylacetylene on the (2×2) alloy surface and 0.14 ML or 58% of the chemisorbed methylacetylene on the $\sqrt{3}$ alloy surface. The number of peaks, peak temperatures, and peak shapes in TPD for the desorption of methylacetylene closely correspond to previous results obtained for the desorption of acetylene from Pt(111) and the Sn/Pt(111) surface alloys [21]. Acetylene is irreversibly adsorbed on Pt(111), but desorbs in three peaks at 350, 440 and 510 K on the (2×2) alloy surface, and a single peak at 365 K on the $\sqrt{3}$ alloy surface.

Fig. 4 shows H_2 TPD spectra following methylacetylene adsorption on Pt(111) and the two Pt–Sn surface alloys for a variety of exposures. On the Pt(111) surface, H_2 desorbs in a series of peaks between 450 and 800 K in TPD. The (2×2) alloy shows a higher temperature onset for H_2 desorption, now in a peak at 505 K, and a higher temperature for the complete dehydrogenation of the surface layer, now extending up to 850 K. The $\sqrt{3}$ alloy shows a new H_2 desorption peak at 370 K, and a higher temperature feature from 490

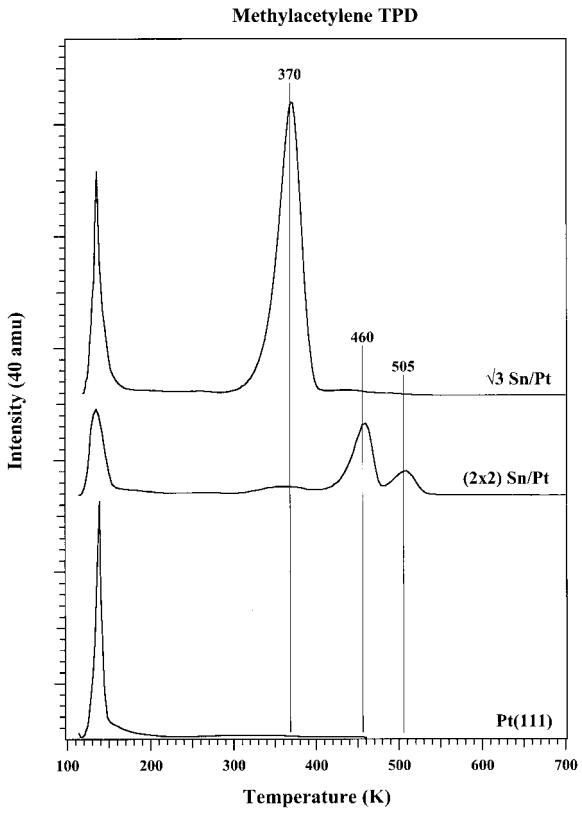

Fig. 3. Methylacetylene TPD spectra after a methylacetylene saturation exposure on the Pt(111), (2×2) and $\sqrt{3}$ Sn/Pt(111) surface alloys at 108 K.

to 850 K. Desorption of H_2 above 400 K is reaction rate-limited and is associated with H_2 produced from the dissociation of methylacetylene. The $\sqrt{3}$ alloy also shows a H_2 desorption peak at 370 K which is desorption rate-limited indicating that on this alloy surface a new pathway for the production of H_2 is created.

The H_2 TPD spectra after methylacetylene exposures yielding a monolayer coverage of methylacetylene on the Pt(111) and Sn/Pt(111) surface alloys, are presented in Fig. 5. In Fig. 5, a constant intensity scale is used for the three surfaces so that the relative areas of the peaks are directly comparable. Hydrogen evolution from the decomposition of methylacetylene is strongly suppressed by alloying Sn in the Pt(111) surface. It is possible to calibrate the areas under the H_2 TPD curves by referencing these to a H_2 TPD curve from a saturation hydrogen coverage obtained by dosing H_2 to the Pt(111) surface at 108 K. Taking the saturation H coverage to be 0.8 ML on Pt(111) [33], it is possible to calculate the amount of H produced from the dissociation of chemisorbed methylacetylene to carbon decreased from 0.68 ML on Pt(111) to 0.24 ML on the (2×2) and 0.04 ML on the $\sqrt{3}$ Sn/Pt(111) alloy surfaces, corresponding to the dissociation of 0.17, 0.06 and 0.01 ML of chemisorbed methylacetylene, respectively.

Increasing the concentration of Sn in the Pt(111) surface also changes the H_2 desorption temperature from dehydrogenation during TPD. The principle peak at 450 K shifts to 505 K and the series of peaks from 500 to 800 K are transformed into a less structured feature that now extends to 850 K upon changing from the Pt(111) surface to the (2×2)-Sn/Pt(111) surface alloy. Increasing the amount of Sn to form the $\sqrt{3}$ surface alloy shifts the peak at 505 K down in temperature to 490 K. Results obtained for D_2 desorption from the dissociation of deuterated acetylene on Pt(111) and the two Sn/Pt(111) surface alloys [21] showed similar behavior. With increasing Sn concentration in this series, the largest D_2 peak shifts from 495 to 515 and then to 490 K, respectively. The desorption of H_2 [33,34] and D_2 [35] following H(D) atom exposure on Pt(111) and the (2×2) and $\sqrt{3}$ surface alloys has been previously studied. The H_2 TPD peaks occur at 380–320, 400–350 and 300 K on the three respective surfaces. Desorption of H_2 associated with the decomposition of methylacetylene (and acetylene) is reaction rate-limited by the breaking of C–H bonds in the molecule.

Post-TPD AES studies of these surfaces are consistent with the H_2 TPD data and show that the amount of carbon produced from dehydrogenation of the monolayer decreases significantly as the concentration of Sn in the surface is increased. The amount of adsorbed methylacetylene which undergoes complete dissociation to form surface carbon on the three surfaces has been determined using as a standard the carbon left on the surface from the decomposition of a saturation coverage of ethylene, that is, $H_C=0.22$ ML [36]. Using this calibration gives $H_C=0.60$, 0.15 and 0.075 after

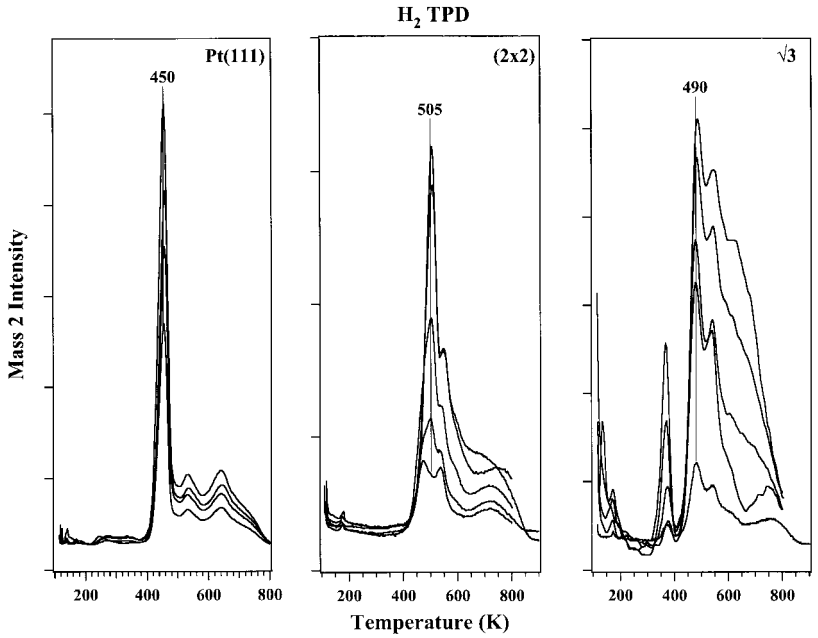

Fig. 4. H_2 TPD for a series of coverages on the Pt(111), (2×2) and $\sqrt{3}$ Sn/Pt(111) surface alloys at 108 K.

TPD on the Pt(111), (2×2) and $\sqrt{3}$ Pt–Sn alloy surfaces, respectively, which corresponds to the complete dehydrogenation of 0.20, 0.05 and 0.025 ML of methylacetylene on these three surfaces. AES reveals that while 76% of the chemisorbed monolayer leads to carbon upon heating on the Pt(111) surface, only 26 and 8% of the chemisorbed monolayer forms carbon on the (2×2) and $\sqrt{3}$ Sn/Pt(111) surface alloys, respectively. The carbon AES signal measures a different value for the amount of methylacetylene decomposition than the H_2 TPD data because a significant portion of the H_2 produced from the decomposition of methylacetylene is consumed in the hydrogenation reactions responsible for the formation of other products (propylene, butene and butane).

3.2. Methylacetylene reactions

The principal desorbed products of the reaction of a monolayer of methylacetylene during TPD on the three surfaces are shown in Figs. 6–8. Along with the TPD spectra presented in Figs. 6–8, signals at 120, 105, 84, 76, 69, 68, 67, 54, 44, 43, 30, 32, 27, 26, 18, 17, 16, 12 and 2 were also monitored during TPD to measure any impurities dosed and possible cyclotrimerization, dehydrogenation and decomposition products. Only those spectra which showed significant desorption signals are reported here. Specifically, the authors tried to detect any cyclotrimerization of methylacetylene to form trimethylbenzene [18] during TPD. No trimethylbenzene was detected under any conditions during TPD on any of the three surfaces. Also, any products that are identified clearly come from the reaction since the yield of these products saturates with increasing methylacetylene doses above the monolayer.

Fig. 6 provides TPD spectra for the principle desorbed products that result from the adsorption of a dose of methylacetylene of slightly >1 ML on Pt(111) at 108 K. The desorption peaks at 130 K are all cracking fractions associated with desorption of the second, physisorbed layer of methylacetylene. Both the molecular methylacetylene (40 amu) and H_2 TPD (2 amu) spectra from Figs. 2 and 4 are reproduced in Fig. 6 for comparison. The primary product is propylene (C_3H_6, 42 amu), which occurs in a broad feature from 270 to 350 K. Independent studies of propylene

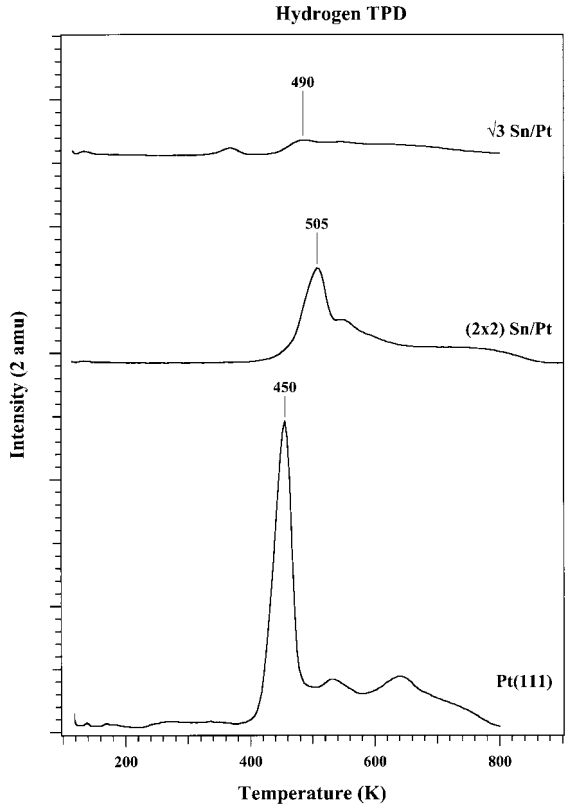

Fig. 5. H_2 TPD spectra after a methylacetylene saturation exposure on the Pt(111), (2×2) and $\sqrt{3}$ Sn/Pt(111) surface alloys at 108 K.

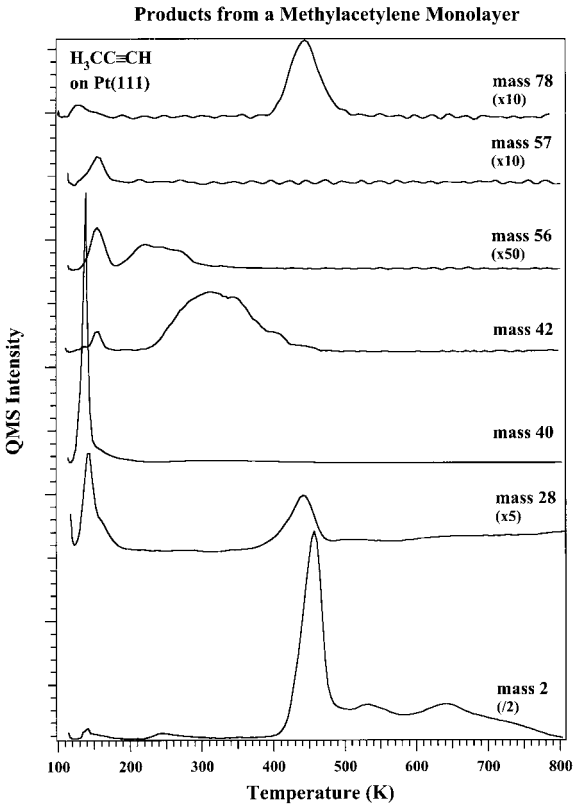

Fig. 6. TPD spectra of products from the reaction of methylacetylene after the adsorption of a coverage slightly greater than 1 ML of methylacetylene dosed at 108 K on the Pt(111) surface.

adsorption on Pt(111) show that propylene is partially reversibly adsorbed, with desorption occurring in a relatively narrow peak that shifts from 284–272 K with increasing coverage [31]. The low temperature side of the propylene desorption feature occurs at about the limit for desorption rate-limited kinetics. However, chemisorbed propylene is completely desorbed by 300 K and so the higher temperature desorption of propylene in Fig. 6 indicates that a portion of the propylene desorption is reaction rate-limited. Some benzene (78 amu) desorbs in a desorption rate-limited peak at 460 K [37], and small desorption signals are detected at 56 and 57 amu. The single sharp peak at 170 K at 57 amu is assigned to butane (C_4H_{10}) desorption. This agrees well with TPD from butane adsorbed on Pt(111) [20]. Desorption rate-limited butane evolution indicates that the Pt(111) surface is very reactive for methylacetylene causing it to dissociate or disproportionate at very low temperatures and that some hydrogenation must be facile and occur below 170 K. The 56 amu desorption signals from 200 to 290 K are assigned to butene and isobutylene (C_4H_8) desorption. This assignment was made primarily by comparisons to the TPD spectra from chemisorbed butene and isobutylene on Pt(111) [31]. Fig. 6 shows that these peaks are desorption rate-limited products from methylacetylene reactions. Finally, a small 28 amu TPD peak at 425 K is assigned to the desorption of ethylene (C_2H_4) from the Pt(111) surface. Chemisorbed ethylene desorbs at 280 K from Pt(111) [31], indicating that ethylene produced from adsorbed methylacetylene desorbs in a reaction rate-limited peak. Because the primary desorption feature occurs at 28 amu, which is also the

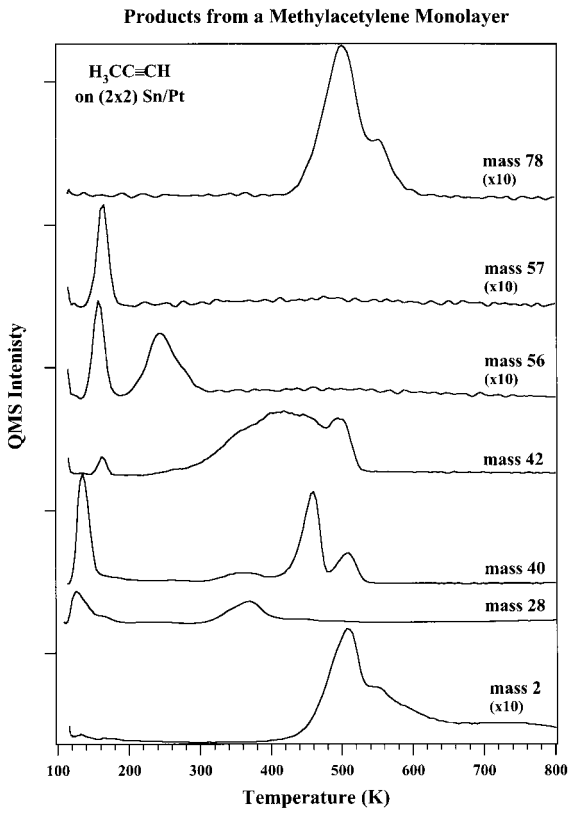

Fig. 7. TPD spectra of products from the reaction of methylacetylene after the adsorption of a coverage slightly greater than 1 ML of methylacetylene dosed at 108 K on the (2×2)Pt–Sn surface alloy.

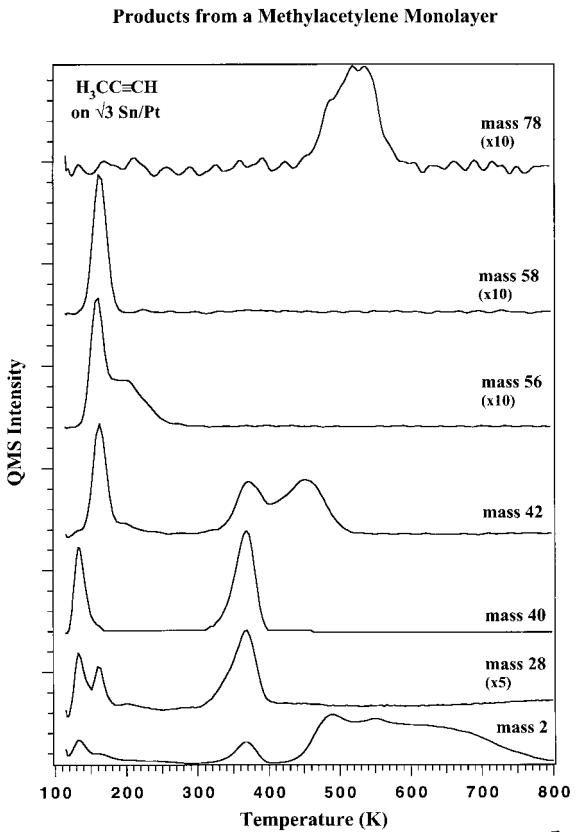

Fig. 8. TPD spectra of products from the reaction of methylacetylene after the adsorption of a coverage slightly greater than 1 ML of methylacetylene dosed at 108 K on the $\sqrt{3}$ Pt–Sn surface alloy.

primary desorption feature of CO it is reasonable to ask about the CO contribution to this spectra. The 26 amu signal was also monitored to insure that this peak was not due to CO and to also detect any desorption of C_2H_2 (no new features were observed).

Fig. 7 shows the TPD spectra of all of the products desorbed following methylacetylene adsorption on the (2×2) alloy. The desorption peaks at 130 K are all cracking fractions associated with desorption of the second physisorbed layer of methylacetylene. The molecular methylacetylene (40 amu) and H_2 (2 amu) TPD spectra from Figs. 2 and 4 are reproduced in Fig. 7 for comparison. A large propylene (42 amu) product desorbs in a series of peaks at 370, 450 and 500 K in TPD. Independent studies of propylene adsorption on the (2×2)Pt–Sn surface show molecular desorption of propylene in a single peak at 232 K [31], indicating that desorption of propylene in Fig. 7 is reaction rate-limited. Benzene (78 amu) desorbs in a peak at 500 K, along with a high temperature shoulder, from the reaction of methylacetylene on the (2×2)Pt–Sn alloy surface. Peaks in TPD in the 56 and 58 amu spectra are assigned to desorption rate-limited evolution of butene and butane, respectively. Butane desorbs in a single sharp peak at 167 K, while butene is observed in a series of peaks from 220 to 260 K. This can be assigned to the production of a mixture of 1-butene, *cis*-2-butene and isobutylene in desorption rate-limited peaks [38]. The peak at 167 K in the butene TPD spectrum is associated with a cracking fraction of

butane. A small reaction rate-limited ethylene (28 amu) product desorbs at 350 K.

Fig. 8 provides TPD spectra of the products formed from the adsorption of slightly greater than 1 ML dose of methylacetylene on the $\sqrt{3}$ alloy. The desorption peaks at 130 K are all cracking fractions associated with desorption of the second, physisorbed layer of methylacetylene. The molecular methylacetylene (40 amu) and H_2 TPD (2 amu) spectra from Figs. 2 and 4 are reproduced in Fig. 8 for comparison. Propylene (42 amu) produced from the reaction of methylacetylene on the $\sqrt{3}$ surface desorbs in two peaks at 360 and 450 K during TPD. These temperatures are significantly higher than that for propylene desorption (180 K) after propylene adsorption on the $\sqrt{3}$ alloy, indicating that the desorption of propylene is reaction rate-limited. TPD also shows the desorption of a benzene (78 amu) product in a broad, reaction rate-limited peak at 550 K. In previous studies of benzene adsorbed on the $\sqrt{3}$ alloy, benzene desorption occurred at 300 K [37]. Butane (58 amu) and butene (56 amu) are also observed during TPD. A single desorption peak at 165 K is assigned to desorption rate-limited butane evolution, while butene desorption occurs in two peaks at 170 and 210 K. The butene produced from the reaction of methylacetylene on the $\sqrt{3}$ alloy surface can be assigned to the desorption rate-limited evolution of a mixture of 1-butene, *cis*-2-butene and isobutylene[38]. The peak at 165 K in the butene TPD spectrum is associated with a cracking fraction of butane. A small reaction rate-limited ethylene (28 amu) peak occurs at 360 K. This ethylene desorption is also coincident with the desorption of methylacetylene, but using data for the methylacetylene cracking fractions on all three surfaces as a standard one can see that this peak cannot be assigned to only a cracking fraction of methylacetylene.

Fig. 9 provides a direct comparison of the desorption of propylene from methylacetylene decomposition on the three surfaces. With increasing Sn concentration, the amount of propylene desorption decreases and the temperature of propylene desorption is strongly shifted to higher temperatures. This shift is not observed in propylene TPD after propylene adsorption on these surfaces, and in contrast the propylene desorption temperature decreases with increased concentration of surface Sn from 272 K on Pt(111), 232 K on the (2×2) alloy, to 180 K on the $\sqrt{3}$ alloy [31]. Clearly desorption of propylene is rate-limited by some surface reaction on the alloys. The correspondence between the desorption temperature of methylacetylene and the onset of propylene desorption on the alloys might indicate that the desorption of methylacetylene frees up sites necessary for the subsequent hydrogenation of methylacetylene. The amount of propylene produced on the three surfaces was determined by comparing the TPD spectrum from a saturation dose of propylene adsorbed on Pt(111). Using this reference standard, methylacetylene decomposition yields 0.056, 0.05 and 0.045 ML of propylene on the three surfaces, respectively.

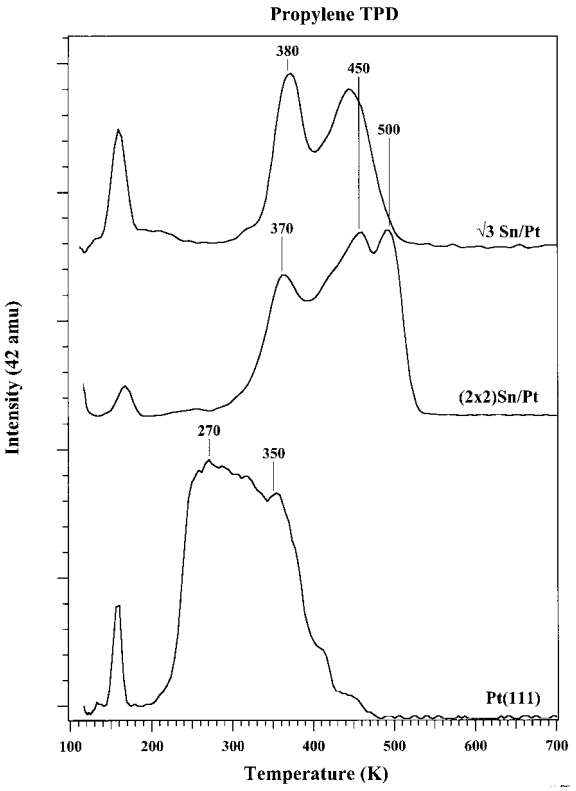

Fig. 9. Propylene TPD spectra after a methylacetylene saturation exposure on the Pt(111), (2×2) and $\sqrt{3}$ Sn/Pt(111) surface alloys at 108 K.

Several minor C_4 products are also formed from the reaction of methylacetylene with Pt(111) and the Sn/Pt(111) surface alloys, and these are directly compared in Fig. 10. Alloying with Sn increases the butane and butene yields, but changing the nature of the alloy has little effect on the amounts of these C_4 products desorbed. Changing the composition of the surface alters the desorption temperatures of both of these products in an understandable way since all of the peaks are desorption rate-limited. The low temperature desorption of butane places an upper limit on the temperature at which C–C bond cleavage of methylacetylene must occur, that is, below 165–170 K. The amount of butane produced by reaction of methylacetylene was determined by dosing a saturation coverage of butane (0.25 ML [20]) on the Pt(111) surface and using the butane (58 amu) area in TPD as a standard. Using this reference, the reaction of methylacetylene forms 0.002, 0.005 and 0.004 ML of butane on the respective surfaces. The amount of these butenes produced during the reaction of methylacetylene was determined by dosing a saturation coverage of 1-butene and isobutylene on the Pt(111) surface. In an independent study of 1-butene, *cis*-2-butene and isobutylene on the Pt(111) surface, the saturation coverages of the molecules were determined to be 0.17, 0.13 and 0.12 ML, respectively. Using these standards the reaction of methylacetylene produces 0.003, 0.009 and 0.006 ML of the butenes on the respective surfaces.

The benzene product desorption curves are compared in Fig. 11. Alloying the Pt(111) surface with Sn pushes up the temperature for forming benzene substantially. Benzene desorbs in a desorption rate

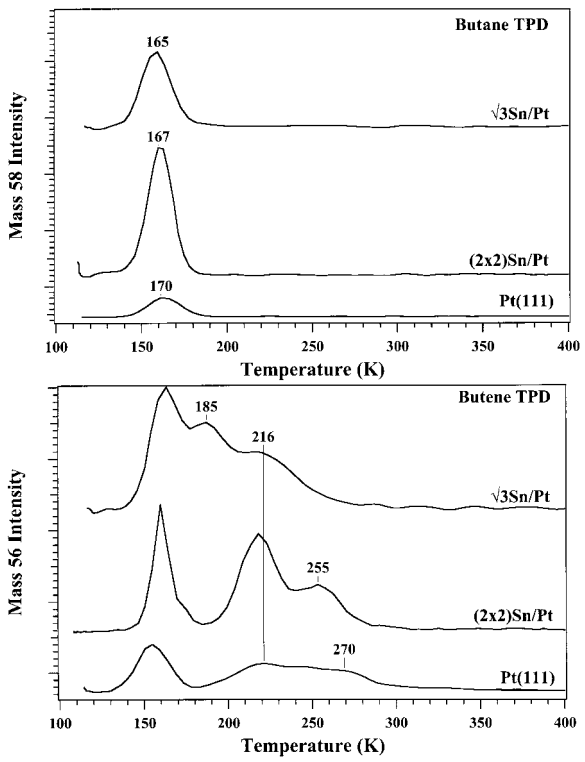

Fig. 10. Butane and butene TPD spectra after a methylacetylene submonolayer and saturation exposure on the Pt(111), (2×2) and $\sqrt{3}$ Sn/Pt(111) surface alloys at 108 K.

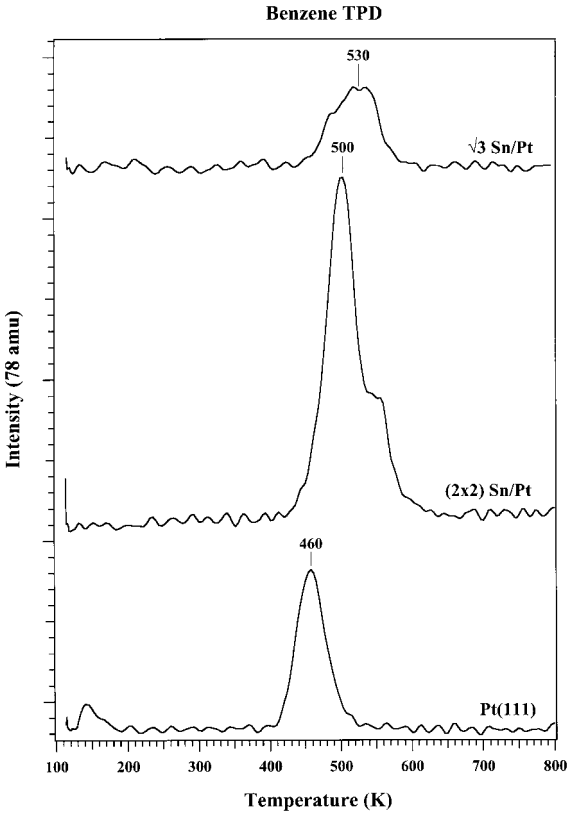

Fig. 11. Benzene TPD spectra after a methylacetylene saturation exposure on the Pt(111), (2×2) and $\sqrt{3}$ Sn/Pt(111) surface alloys at 108 K.

limited peak at 460 K on Pt(111), but desorbs at higher temperatures in reaction rate limited peaks on the two alloys, with no major influence of the Sn composition on the desorption temperature. The alloy composition has an influence on the amount of benzene product desorbed, with the (2×2) alloy showing the largest yield. Using the benzene TPD areas in Fig. 11 and comparing those to a calibration measurement of the benzene TPD area from a saturation coverage (0.1 ML [37]) of benzene on Pt(111), it is possible to estimate the amount of benzene formed by the reaction of methylacetylene to be 0.0056, 0.008 and 0.0025 ML on the Pt(111), (2×2) and $\sqrt{3}$ Pt–Sn alloy surfaces, respectively.

Determining the relative importance of the various reaction pathways on the three surfaces is a key issue. This involves calibration of the relative amounts of methylacetylene consumed to yield each product. Using some reasonable assumptions, and recalling that the initial coverage in the chemisorbed methylacetylene monolayer on each of the surfaces is the same at 0.25 ML, the estimates summarized in Fig. 12 can be made. Earlier, it was determined that $H_C=0.60$, 0.15 and 0.075 after TPD on the Pt(111), (2×2) and $\sqrt{3}$ Pt–Sn alloy surfaces, respectively, and thus the amount of adsorbed methylacetylene that undergoes complete dissociation to form surface carbon on the three surfaces is 0.20, 0.05 and 0.025 ML on these three surfaces. AES revealed that while 76% of the chemisorbed monolayer leads to carbon upon heating on the Pt(111) surface, only 26 and 8% of the chemisorbed monolayer forms carbon on the (2×2) and $\sqrt{3}$ Sn/Pt(111) surface alloys, respectively. Because the carbon number in propylene and methylacetylene are the same, it is assumed the amount of propylene desorbed also corresponds to the amount of methylacetylene consumed. Thus, 22, 20 and 18% of the chemisorbed monolayer of methylacetylene is converted into propylene on the three surfaces, respectively. The butane and butene yields correspond very roughly (simply assuming ratios according to the carbon numbers) to the conversion of 0.003, 0.007 and 0.005 ML methylacetylene to butane, or 0.9, 2.8 and 1.9% of the chemisorbed monolayer of methylacetylene to butane, and the conversion of 0.004, 0.012 and 0.008 ML methylacetylene to butene, or 1.5, 4.7 and 3.2% of the chemisorbed monolayer of methylacetylene to butene, for the Pt(111), (2×2) and $\sqrt{3}$ surface, respectively. The benzene formed accounts for the conversion of 0.005, 0.016 and 0.011 ML methylacetylene, or 4.5, 6.3 and 2% of the chemisorbed monolayer of methylacetylene, for the Pt(111), (2×2) and $\sqrt{3}$ surfaces, respectively. There is a reasonable mass balance for Pt(111), and obviously molecular methylacetylene desorption should account for the balance of the fate of the chemisorbed layer on the alloys. About 26% of the chemisorbed methylacetylene on the (2×2) alloy desorbs in TPD, while 58% of the chemisorbed methylacetylene on the $\sqrt{3}$ alloy desorbs in TPD.

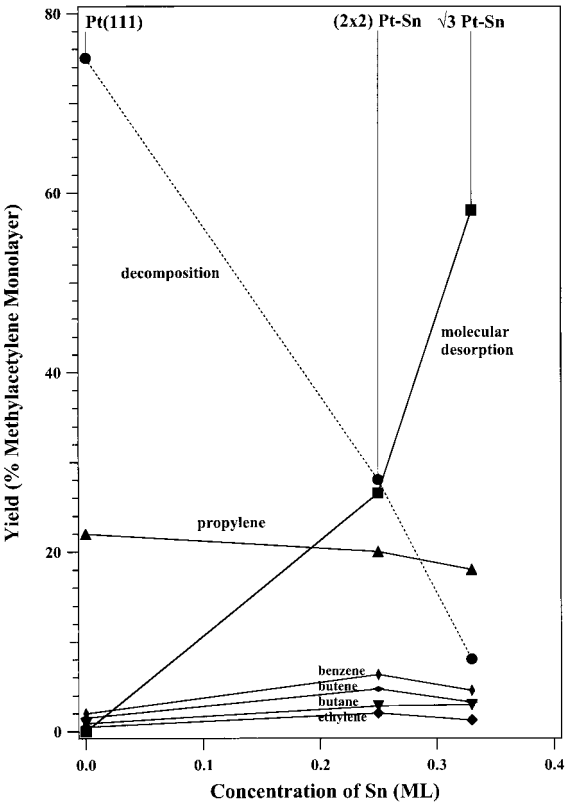

Fig. 12. A quantitative comparison of the relative yields of the major products on the Pt(111), (2×2) and $\sqrt{3}$ Sn/Pt(111) surface alloys at saturation coverages.

4. Discussion

It was found that methylacetylene is very reactive and irreversibly adsorbed on Pt(111). Post-TPD AES studies show that 76% of the adsorbed layer undergoes decomposition to form carbon. About 22% of the remaining methylacetylene undergoes hydrogenation to form propylene. The remaining chemistry involves dimerization to form benzene and C–C bond cleavage to form butane, butene and ethylene, although this chemistry accounts for $<6\%$ of the adsorbed monolayer of methylacetylene.

Alloying Sn to form the Pt–Sn surface alloys decreases the complete dehydrogenation of methylacetylene to form surface carbon, as shown in Fig. 12, and causes a large increase in the amount of reversibly adsorbed methylacetylene (26 and 58% of the adsorbed layer on the 2×2 and $\sqrt{3}$ alloys, respectively). This is at least partly due to a decreased adsorption energy for methylacetylene as the Sn concentration increases, from ca 38.5 kcal mol^{-1} [39] on Pt(111), to 28.5 kcal mol^{-1} on the (2×2) alloy, to 23 kcal mol^{-1} on the $\sqrt{3}$ alloy. Interestingly, the propylene yield (18–20% of the adsorbed layer) is nearly insensitive to the Sn concentration in the surface layer. The other reaction products, that is, butene, butane, benzene and ethylene show a somewhat higher yield on the (2×2) alloy compared to the other surfaces. So, methylacetylene adsorption on the two alloys leads primarily to methylacetylene desorption and some propylene desorption.

An important comparison to make is that of acetylene adsorption and reaction on Pt(111) and these two surface alloys [21]. On Pt(111), heating the surface after acetylene adsorption leads to surface carbon and H_2 desorption. Between 330 and 400 K, adsorbed acetylene undergoes a bimolecular disproportionation reaction to form ethylidyne and ethynyl [3], which decomposes further to give a large H_2 TPD peak at 495 K and complete dehydrogenation by 800 K. Alloying Sn decreased the amount of acetylene that formed surface carbon from 98% on Pt(111), to 70 and 35% on the two respective alloys. This decreased reactivity was accompanied by in increase in the amount of reversible acetylene adsorption, from 2% on Pt(111), to 11 and 55% on the two respective alloys. The acetylene adsorption energy is decreased from ca 38.5 kcal mol^{-1} [21] on Pt(111), to 28.5 kcal mol^{-1} on the (2×2) alloy, to 23 kcal mol^{-1} on the $\sqrt{3}$ alloy [21]. The most interesting result of alloying Sn is to open a new reaction pathway for forming gas phase benzene. Butadiene desorption was also observed. Based on the previous work of Lambert and coworkers [7–18], it is proposed that acetylene undergoes a dimerization reaction to form a metallocyclopentadiene intermediate which can either be hydrogenated and desorbed into the gas phase as butadiene or can add another acetylene to give a net cyclotrimerization reaction to form benzene. The $\sqrt{3}$ alloy produced the most gas phase benzene in TPD, and the amount was estimated to correspond to ca 10% of the chemisorbed acetylene.

The adsorption energies of methylacetylene and acetylene are essentially the same, and the reactivity of these two molecules follow the same general trends on the three surfaces. For example, the production of H_2 (from 70% on Pt(111) to as little as 8% on the $\sqrt{3}$ alloy) and surface carbon from decomposition of methylacetylene is decreased and the amount of reversible molecular desorption of methylacetylene (from no molecular desorption on Pt(111) to 58% on the $\sqrt{3}$ alloy) is increased as Sn is alloyed. However, the gas phase products that desorb from methylacetylene and acetylene reactions are dramatically different. Most notably adsorbed acetylene undergoes dimerization and cyclotrimerization to form benzene, while methylacetylene does not produce any hydrogenated dimer products (C_6 open-chain dienes) or form trimethylbenzene. Hydrogenation dominates methylacetylene reactions, in contrast to acetylene where no ethylene is desorbed. C–C and C–H bond cleavage occurs at very low temperatures (below 170 K) as evidenced by desorption of butene and butane.

These different reaction pathways are the result of the methyl group in methylacetylene. While the H_3C–CCH bond is the weakest bond in the molecule (90 kcal mol^{-1} [40]), the most facile bonds are typically C–H bonds and methylacety-

lene has a 43.5 kcal mol^{-1} weaker bond, D(H–CH_2CCH) = 89.4 kcal mol^{-1}, than does acetylene with D(H–CCH) = 132.9 kcal mol^{-1}! This lability generates surface hydrogen at much lower temperatures for methylacetylene than in the case of acetylene, and this can account for the large propylene production. If dehydrogenation occurs prior to dimerization, then an adsorbed $\dot{C}H_2$–C≡CH intermediate might be formed, and this species could also isomerize to CH_2=C=C$\dot{H}$. (These species are covalently bonded to the surface by one Pt–C s bond at a terminal carbon, as indicated by the radical site, and further coordinated to the surface through bonding interactions with the triple or double bonds present initially in the molecules.) Neither of these intermediates, nor the allene CH_2=C=CH_2 that would be formed by a 1,3-H shift in methylacetylene, should lead to the dimethyl-substituted metallocyclopentadiene intermediate expected by analogies to acetylene chemistry. So one never observes any hydrogenated dimer products (C_6 open-chain dienes) and further the even higher temperature process of insertion of a third methylacetylene to form trimethylbenzene never occurs. Minor pathways that produce benzene and the C_4 products must also be accounted for, even though it is not easy to understand. Benzene could be formed via dimerization of methylacetylene, or any of the C_3 intermediates mentioned already, and subsequent dehydrogenation. Benzene desorption occurs at quite high temperatures (460–530 K) and condensation reactions can certainly occur at such temperatures. Production of the C_4 species must involve C–C bond cleavage (either dissociation to produce adsorbed C_1 species or methyl transfer in disproportionation reactions) at very low temperatures, with an activation energy of ~10 kcal mol^{-1}, since a pathway of dimerization followed by elimination of C_2 would seemingly be a more highly activated process. Methyl group transfer, analogous to the hydride transfer in the disproportionation of acetylene that occurs at 330 K as noted already, may be possible at such low temperatures given the large (43 kcal mol^{-1}) difference in the H_3C–CCH and H–CCH bonds. An understanding of the reaction mechanism must await further and more detailed analysis perhaps using high resolution electron energy loss spectroscopy (HREELS) or Fourier transform infrared (FTIR) spectroscopy and isotope labeling experiments.

Finally, this chemistry differs from that seen in reactions of methylacetylene on TiO_2 under UHV conditions [18]. During TPD, ca 76% of the methylacetylene monolayer underwent cyclotrimerization to form trimethylbenzene, 17% formed propylene, and most of the remaining methylacetylene formed dimerized products such as 2,3-dimethyl-1,3-butadiene, 2,4-hexadiene and 2-methyl-1,3-pentadiene. Only a small fraction of reversibly adsorbed methylacetylene and no carbon due to complete dehydrogenation was seen. TiO_2 also showed increased selectivity for methylacetylene cyclotrimerization (76%) compared to acetylene cyclotrimerization (51%). The observation of significant propylene production on TiO_2 indicates that the hydrogenation of methylacetylene is a facile and fairly general reaction for this molecule. These authors also discuss the role of isomerization of methylacetylene to allene (H_2C=C=CH_2). Allene does not lead to cyclotrimerization, and perhaps it is a facile conversion of methylacetylene to allene on metal surfaces that lowers the cyclotrimerization yield.

5. Conclusions

Alloying Sn in the Pt(111) surface to form two ordered surface alloys strongly decreases the reactivity of methylacetylene on the Pt(111) surface. On Pt(111), methylacetylene adsorption is completely irreversible and ca 80% of the chemisorbed layer completely dehydrogenates to form surface carbon. The main reaction product desorbed is propylene, and ca 20% of the adsorbed methylacetylene layer desorbs as propylene. Alloying Sn to form the Pt–Sn surface alloys does not alter the coverage in the chemisorbed layer, but caused a large increase in the amount of reversibly adsorbed methylacetylene (25–60% of the adsorbed layer desorbs as methylacetylene) and a large decrease in the complete dehydrogenation of methylacetylene to form surface carbon. Propylene is the other major hydrocarbon product desorbed (18–20% of

the adsorbed layer), and the amount is nearly insensitive to the Sn concentration in the surface layer. On all three surfaces, a small concentration of other reaction products, that is, butene, butane and ethylene were observed and these give some evidence for low temperature reactions involving C–C bond breaking below 170 K. Methylacetylene is much more weakly adsorbed on the alloys than Pt(111), and the methylacetylene adsorption energy is 28.5 kcal mol^{-1} on the (2×2) alloy and 23 kcal mol^{-1} on the $\sqrt{3}$ alloy, compared to an estimated 38.5 kcal mol^{-1} on Pt(111). While acetylene is known to cyclotrimerize to form and desorb benzene on these Pt–Sn alloys, no cyclotrimerization of methylacetylene to form trimethylbenzene was observed. It is proposed that this is primarily due to the weak $H–CH_2CCH$ bond in methylacetylene ($\sim$89 kcal mol^{-1}) which undergoes reaction to form intermediates that are more difficult to dimerize and cyclotrimerize and also populates the surface with a relatively large amount of adsorbed hydrogen at low temperatures that can lead to propylene formation. A small amount of benzene desorption (2–6%) was observed from methylacetylene reactions on all these surfaces at relatively high temperature (460–530 K) from condensation reactions that take place under these conditions.

Acknowledgements

This work was partially supported by the Division of Chemical Sciences, Office of Basic Energy Sciences, U.S. Department of Energy. J.W.P. would like to thank the Department of Education for a graduate research fellowship.

References

[1] M. Berthelot, Ann. Chem. 141 (1867) 353.
[2] J.C. Bertolini, J. Massardier, G.J. Dalmai-Imelik, J. Chem. Soc. Faraday Trans. 74 (1978) 1720.
[3] N.R. Avery, J. Am. Chem. Soc. 107 (1985) 6711.
[4] W.T. Tysoe, G.L. Nyberg, R.M. Lambert, J. Chem. Soc., Chem. Commun. (1983) 623.
[5] W.T. Tysoe, G.L. Nyberg, R.M. Lambert, Surf. Sci. 135 (1983) 128.
[6] W. Sesselmann, B. Woratschek, G. Ertl, J. Kuppers, Surf. Sci. 130 (1983) 245.
[7] T.M. Gentle, E.L. Muetterties, J. Phys. Chem. 87 (1983) 2469.
[8] B. Marchon, Surf. Sci. 162 (1985) 382.
[9] T.G. Rucker, M.A. Logan, T.M. Gentle, E.L. Muetterties, G.A. Somorjai, J. Phys. Chem. 90 (1986) 2703.
[10] J.P. Collman, L.S. Hegedus, J.R. Norton, R.G. Finke, in: Principles and Applications of Organtransition Metal Chemistry, 2nd ed., University Science Books, Mill Valley, CA, 1987, p. 870.
[11] C.H. Patterson, R.M. Lambert, J. Phys. Chem. 92 (1988) 1266.
[12] C.H. Patterson, J.M. Mundenar, P.Y. Timbrell, A.J. Gellman, R.M. Lambert, Surf. Sci. 208 (1989) 93.
[13] H. Hoffmann, F. Zaera, R.M. Ormerod, R.M. Lambert, P. Wang, W.T. Tysoe, Surf. Sci. 232 (1990) 259.
[14] R.M. Ormerod, R.M. Lambert, Catal. Lett. 6 (1990) 121.
[15] R.M. Ormerod, R.M. Lambert, J. Chem. Soc., Chem. Commun. (1990) 1421.
[16] R.M. Lambert, R.M. Ormerod, Mater. Chem. Phys. 29 (1991) 105.
[17] R.M. Ormerod, R.M. Lambert, J. Phys. Chem. 96 (1992) 8111.
[18] K.G. Pierce, M.A. Barteau, J. Phys. Chem. 98 (1994) 3882.
[19] M.T. Paffett, S.C. Gebhard, R.G. Windham, B.E. Koel, Surf. Sci. 223 (1989) 449.
[20] C. Xu, B.E. Koel, M.T. Paffett, Langmuir 10 (1994) 166.
[21] C. Xu, J.W. Peck, B.E. Koel, J. Am. Chem. Soc. 115 (1993) 751.
[22] C. Xu, T.-L. Tsai, E.B. Koel, J. Phys. Chem. 98 (1994) 585.
[23] C. Xu, B.E. Koel, Surf. Sci. 292 (1993) L803.
[24] C.T. Campbell, G. Ertl, H. Kuipers, J. Segner, Surf. Sci. 107 (1981) 220.
[25] M.T. Paffett, R.G. Windham, Surf. Sci. 208 (1989) 34.
[26] M.T. Paffett, S.C. Gebhard, R.G. Windham, B.E. Koel, Surf. Sci. 223 (1989) 449.
[27] S.H. Overbury, D.R. Mullins, M.T. Paffet, B.E. Koel, Surf. Sci. 254 (1991) 45.
[28] A. Atrei, U. Bardi, J.X. Wu, E. Zanazzi, G. Rovida, Surf. Sci. 290 (1993) 286.
[29] M. Galeotti, A. Atrei, U. Bardi, G. Rovida, M. Torrini, Surf. Sci. 313 (1994) 349.
[30] R.L. Summers, NASA Technical Note TN D-5285, NASA, Lewis Research Center, Cleveland, OH, 1969.
[31] Y.-L. Tsai, C. Xu, B.E. Koel, Surf. Sci. 385 (1997) 37.
[32] P.A. Redhead, Vacuum 12 (1962) 203.
[33] M.T. Paffett, S.C. Gebhard, R.G. Windham, B.E. Koel, J. Phys. Chem. 94 (1990) 6831.
[34] S.C. Gebhard, B.E. Koel, J. Phys. Chem. 96 (1992) 7056.
[35] M. Voss, H. Busse, B.E. Koel, to be published.
[36] R.G. Windham, M.E. Bartram, B.E. Koel, J. Phys. Chem. 92 (1988) 2862.
[37] C. Xu, B.E. Koel, Surf. Sci. 304 (1994) 249.
[38] Y.-L. Tsai, B.E. Koel, J. Phys. Chem. B. 101 (1997) 2895.
[39] M.E. Bartram, B.E. Koel, E.A. Carter, Surf. Sci. 219 (1989) 467.
[40] C.T. Mortimer, Reaction Heats and Bond Strengths, Pergamon Press, New York, 1962.